Title
THE PRODUCTION OF CHARGED PHOTOMESONS FROM DEUTERIUM AND HYDROGEN

Authors
White, R. Stephen
Jakobson, Mark J.
Schulz, Alvin G.

Publication Date
1952-03-28

UNIVERSITY OF CALIFORNIA — BERKELEY

RADIATION LABORATORY

DISCLAIMER

UCRL-1319 Rev.
Unclassified

UNIVERSITY OF CALIFORNIA

Radiation Laboratory

Contract No. W-7405-eng-48

THE PRODUCTION OF CHARGED PHOTOMESONS FROM DEUTERIUM AND HYDROGEN--PART I

R. Stephen White, Mark J. Jakobson, and Alvin G. Schultz

March 28, 1952

Berkeley, California

THE PRODUCTION OF CHARGED PHOTOMESONS FROM DEUTERIUM AND HYDROGEN--PART 1*

R. Stephen White, Mark J. Jakobson†, and Alvin G. Schulz††

Radiation Laboratory, Department of Physics
University of California, Berkeley, California

ABSTRACT

Hydrogen and deuterium gases have been bombarded in a gas target at a temperature of 77°K and at a pressure of about 140 atmospheres by the 318 ± 10 Mev "spread-out" bremsstrahlung photon beam of the Berkeley electron synchrotron. The charged π mesons which were produced were collimated at angles of 45°, 90°, and 135° to the beam direction. The π^+ mesons were detected with trans-stilbene scintillation crystals using $\pi\mu$, $\pi\beta$, and $\pi\mu\beta$ delayed coincidences and π^+ and π^- mesons were detected with Ilford C-2 200 micron nuclear emulsions. The ratios of the numbers of π^- to π^+ mesons produced in deuterium were 0.96 ± 0.10, 1.09 ± 0.12 and 1.21 ± 0.17 for the angles of 45°, 90°, and 135°, respectively. No variation of the ratio with meson energy, outside statistics, was observed. Absolute values for the π^+ meson energy distribution functions from hydrogen and deuterium per "equivalent quantum" have been measured at each of the above production angles. The differential and total cross sections have been obtained by integrating over energy and angle, respectively. The experimental ratios of the deuterium to hydrogen cross sections are in good agreement with the phenomenological theory of Chew and Lewis when the Hulthén deuteron function with $\beta = 6\alpha$ is used in the initial state, plane waves are used for the nucleons in the final state, and the bremsstrahlung cut-off is taken into account. The statistics of the data are, however, not sufficient to determine the amount of spin interaction. The excitation functions for hydrogen and deuterium and points on the angular distribution curves in the center of mass system have been obtained. An upper limit of 0.08 of the charged π meson cross section was obtained for μ meson production from deuterium.

---

*Part 2 of this paper will be The Production of Charged Photomesons from Helium. Helium-hydrogen Ratios.

†Now at University of Washington, Seattle, Washington
††Now at Applied Physics Laboratory, Johns Hopkins University, Silver Springs, Maryland

THE PRODUCTION OF CHARGED PHOTOMESONS FROM DEUTERIUM AND HYDROGEN--PART 1

R. Stephen White, Mark J. Jakobson, and Alvin G. Schulz

Radiation Laboratory, Department of Physics
University of California, Berkeley, California

I. INTRODUCTION

Since the first report of photomeson production[1], a number of photomeson production experiments have been performed[2]. It is quite probable that production experiments with nuclei of a large number of nucleons yield more information about the structure of the nucleus, and the meson interaction with nucleons before leaving the nucleus, than about the initial production of the meson itself. For information concerning the production, therefore, experiments with light nuclei should be performed. Of the light nuclei the photomeson production from the free proton or neutron should be the easiest to interpret theoretically because of the absence of nucleon-nucleon interaction complications. These free nucleon reactions are thought to be:

$$\gamma + p \longrightarrow n + \pi^+$$

$$\gamma + n \longrightarrow p + \pi^-$$

The first reaction has been studied by Steinberger, Bishop, and Cook[2c,d,e] and by Feld et al.[2j], and the second has not been investigated because of the lack of a concentrated target of neutrons. As an alternative to the free nucleon reactions, this experiment has utilized the loosely bound neutron and proton in

1. E. M. McMillan and J. M. Peterson, Science 109, 438 (1949)

2a. E. McMillan, J. M. Peterson and R. S. White, Science 110, 579 (1949)
b. J. Peterson, W. Gilbert, and R. S. White, Phys. Rev. 81, 1003 (1951)
c. J. Steinberger and A. S. Bishop, Phys. Rev. 76, 494 (1950)
d. A. S. Bishop, J. Steinberger and L. Cook, Phys. Rev. 80, 291 (1950)
e. J. Steinberger and A. S. Bishop, Phys. Rev. 86, 180 (1952)
f. R. F. Mosley, Phys. Rev. 80, 493 (1950)
g. R. M. Littauer and D. Walker, Phys. Rev. 82, 746 (1951)
h. M. Camac, D. R. Corson, R. M. Littauer, A. M. Shapiro, A. Silverman, R. R. Wilson, W. M. Woodward, Phys. Rev. 82, 745 (1951)
i. H. A. Medicus, Phys. Rev. 83, 662 (1951)
j. B. T. Feld, D. H. Frisch, I. L. Lebow, L. S. Osborne, and J. S. Clark, Phys. Rev. 85, 660 (1952)
k. I. L. Lebow, B. T. Feld, D. H. Frisch, and L. S. Osborne, Phys. Rev. 85, 601 (1952)

the deuteron to compare the above production cross sections. In addition, by comparing the cross sections for the production of π^+ mesons from deuterium and hydrogen one can study the reduction in the deuteron cross section which results from exclusion effects which was first pointed out by Feshbach and Lax.[3a,b] In the deuteron reaction

$$\gamma + d \longrightarrow 2n + \pi^+$$
$$\longrightarrow 2p + \pi^-$$
$$^3S \quad {}^1S \; {}^3P \ldots\ldots$$

as the final nucleon state must be antisymmetric, the resulting neutrons or protons can only end in the ^1S, ^3P,.....states. Since the deuteron is initially in the ^3S state, unless the proton flips its spin in the production of a meson, the available phase space is reduced relative to that for the production from a free proton, or neutron. Chew and Lewis[4] have pointed out that in addition to the above effect the cross section will be further reduced because of the reduction in phase space due to the binding energy of the deuteron. Using a phenomenological approach, they have calculated the ratio of the production cross sections from the deuteron and the proton. Two constants, the amplitude for spin flip and amplitude for non-spin flip appear which can be determined experimentally by a measurement of these cross sections. This problem has also been

---

3a. H. Feshbach and M. Lax, Phys. Rev. 76, 134 (1949)

b. H. Lax and H. Feshbach, Phys. Rev. 81, 189 (1951)

4a. C. F. Chew and H. W. Lewis, Phys. Rev. 84, 779 (1951). For the initial deuteron state, the Hulthén wave function was used. Integration over the final nucleon states was carried out by means of Closure Theorems.

b. C. F. Chew and H. W. Lewis, Unpublished calculations. For the initial deuteron state the Hulthén wave function was used. In the final state the nucleons were treated as plane waves.

treated phenomenologically by other theoretical investigators[5].

An exploratory experiment of Mozley and White[6], using light and heavy water targets and electronic meson detection indicated that π^+ meson production from deuterium, at a production angle of 90°, did not differ greatly from the π^+ meson production from hydrogen. The present experiment was designed to investigate the production of π^+ and π^- mesons from deuterium as a function of both angle of emission and meson energy, and to measure the ratios of the production cross sections for π^+ mesons from deuterium and hydrogen.* This study has also been made by Lebow, Feld, Frisch and Osborne.[2k]

II. EXPERIMENTAL PROCEDURE

The source of photons for this experiment was the 318 ± 10 Mev bremsstrahlung "spread-out" beam from the Berkeley electron synchrotron. This beam was generated from the 322 ± 5 Mev electron beam which struck an internal 0.020 inch platinum target. The "spread-out" beam was obtained by modulating the rf accelerating voltage such that the electrons spilled into the target over a period of about 3,000 μsec.[7] This occurred in such a way that about half of the electrons hit the target before and after the peak field was reached. The emerging beam had a

---

5a. G. Morpurgo, Il Nuovo Cimento 8, 552 (1951). For the initial deuteron state the ordinary exponential wave function was used. In the final state the nucleons were treated as plane waves.

b. S. Machida and T. Tamura, Progress of Theoretical Physics 6, 572 (1951). Calculations are applicable only if the two nucleons end in the ^1S state. For the initial deuteron state the Hulthén wave function was used.

c. Y. Saitō, Y. Watanabe, and Y. Yamaguchi, Progressof Theoretical Physics 7, 103 (1952). For the initial deuteron state the Hulthén wave function was used. In the final state the nucleons were treated as plane waves, as well as distorted S-state waves. The results of their plane wave calculation are equivalent to those of Chew and Lewis[4b].

6. R. F. Mozley and R. S. White, unpublished results.

* Preliminary results of this experiment have previously been reported.
R. S. White, UCRL-1319 (1951).
R. S. White, M. J. Jakobson, and A. G. Schulz, Phys. Rev. 85, 770 (1951)

7. G. Gauer and C. Nunan, UCRL-714 (1950)

full width at half-intensity of 0.0135 radians. At 55 inches from the electron target, the beam was defined by a three-quarter inch tapered hole in a nine-inch lead wall, as in shown in Fig. 1. Two secondary collimators were used to absorb the spray of electrons from the walls of the primary collimator.

The beam was monitored by means of an ionization chamber placed in front of the primary collimator. A second ionization chamber placed ten feet behind the rear end of the target was used as a check on the front monitor. The mesons passed through lead absorbers, were stopped, and were detected either in nuclear emulsions or in trans-stilbene crystal detectors. The nominal detection angles of 45°, 90°, and 135° were defined by uranium slits. Lead shielding served to prevent electrons and mesons, which were emitted at other angles, from reaching the detectors.

A. Target

A high-pressure, low-temperature target was selected for this experiment. The assembly of the target is shown in Fig. 2. The target consisted essentially of 3 concentric cylindrical containers. The inside pressure vessel was designed to withstand a pressure of about 5 times the operating pressure of 140 atmospheres at the operating temperature of 77°K, and was tested to 2 times this operating pressure. The liquid nitrogen made direct contact with the pressure wall for most of the length of the target. The vacuum system was for the purpose of lowering heat conduction to the target gas and for conserving the liquid nitrogen.

The liquid nitrogen was stored in a tank above the target and fed to the cooling wall through pipes. Two thermocouples were placed in the tank at different levels and a third was placed on one of the end caps. The signals were sent to an automatic recorder in the counting area so that one had a record of the nitrogen level and the temperature of the pressure wall, and thus the gas, at all times.

One tube from the gas pressure cylinder was led directly to the counting area to a calibrated pressure gauge. From this gauge the pressure of the gas was read at intervals. The densities of the gases were obtained from the experi-

mental curves for the equations of state measured by Johnston et al.[8] Their values are given to 0.1 percent accuracy.

An oil pump was used to compress the hydrogen gas from cylinder pressure to the operating pressure. Because of the expense of the deuterium it was necessary to recover it after each bombardment. The oil pumping system of Panofsky, et al.[9] was used for this purpose. The pressure system was pumped down to less that 1 mm of Hg pressure in each gas exchange to insure negligible mixing of the gases. When comparison among gases was desired at least three changes of the gases were made in each 16 hour bombardment period.

The photon beam traversed 0.89 gm per cm^2 of stainless steel in the front end of the target and 5.2 gm per cm^2 of the deuterium from the front to the rear of the target. The 5 percent photon attenuation in the stainless steel target end was negilgible compared to the uncertainty in the absolute beam monitoring of 20 percent. The 2 percent attenuation over the entire length of the target gas that might affect the relative values between the 135° and 45° angles is considerably less than the statistics, and is of the same order of accuracy as the relative beam monitoring.

Mesons which were produced in the gas of the target and were emitted perpendicular to the axis of the target had to penetrate 2.3 gm of stainless steel and 0.1 gm of liquid nitrogen. The minimum energy of π mesons that could penetrate this material was 22 Mev; at 45° and 135° the minimum meson energy was 27 Mev. The energy loss of π mesons originating on the center line of the target is less than one Mev in the target gas for all but the lowest energy mesons. This gives a maximum uncertainty in the meson energy, due to the target diameter,

---

8. H. L. Johnston, I. Bezman, T. Rubin, C. Swanson, W. Corak and E. Rifkin, MDDC-850

9. W. Panofsky, L. Aamodt and J. Hadley, Phys. Rev. 81, 565 (1951)

of less than 2 Mev. This uncertainty is small compared to the detector energy widths which ranged from 5 to 20 Mev. For the experimental arrangement used, computations showed that the target could be treated as a line source to within 1 percent accuracy.

Mass spectrometer analysis of the deuterium gas showed a 99 percent concentration of deuterium with about a 1 percent contamination of hydrogen.[10] This amount of contamination could be neglected.

B. Collimators, Slits, and Absorbers

The selection of a gas pressure target with its inherently thick walls required that the target be long so that mesons made in the stainless steel end walls could be shielded out; otherwise, a large subtraction would have been necessitated. Lead was selected for the shielding material as it has a high nuclear charge, Z, and consequently is quite effective in stopping electrons and photons in the bremsstrahlung and pair production region.

Two sections through the meson collimating system are illustrated schematically in Fig. 3. In the section perpendicular to the photon beam direction, at the center of the target, are shown the five similar collimating systems arranged azimuthally about the beam direction. The lower collimating system was used only for the coincidence crystal detectors. The other four identical collimating systems, which were used for the nuclear emulsion detection, allowed the simultaneous measurement of four different energies at each of the three angles of observation.

The angles, as defined by the slits, are shown in the plane section through one of the collimating systems in Fig. 3 and are listed in Table I.

---

10. R. H. Phillips, Private Communication

Table I. Angular Resolution of the Collimating Systems

DETECTOR	LAB ANGLE
NUCLEAR EMULSIONS	$45^{\circ} +17^{\circ} -15^{\circ}$ $90^{\circ} \pm 16^{\circ}$ $135^{\circ} +15^{\circ} -17^{\circ}$
CRYSTALS	$90^{\circ} \pm 16^{\circ}$ $135^{\circ} \pm 19^{\circ}$

From the emulsion data one can obtain a check on the collimation. The channel resolution was folded into the multiple scattering for the mesons passing through the lead and glass absorbers to obtain a distribution in angle of the mesons near their endings. In Fig. 4, for the 45° and 90° collimators, the computed curve for mesons with an initial energy of 70 Mev and final energy of 2 Mev is compared with a set of selected mesons with an average initial energy of 70 Mev. The angle to the collimator direction was measured at 200 microns (2 Mev) back from the meson endings. The calculations of multiple scattering included energy loss in the absorbers.[11]

In order to minimize slit penetration, uranium slits, with a high stopping power per unit length, were used. The low-energy gammas from the uranium did not contribute appreciably to the single-grain background on the nuclear emulsions, nor to the background counts in the crystals.

The part of the emulsion which was scanned and most of the crystal in which the mesons stopped were so placed that very few electrons or mesons could be reflected at small angles off the slits into the detectors. The slit was cut away

---

11. L. Eyges, Phys. Rev. 74, 1535 (1948)
L. L. Foldy, Phys. Rev. 75, 311 (1949)

on the side nearest the detector, so that only electrons or mesons reflected from it at large angles could reach the detectors.

Lead was selected for the absorber material. Lead has a large stopping power per unit length and in addition had a large attenuation for the high energy electrons which were made in the ends of the stainless steel envelope and were scattered down the channels from the cylindrical walls of the target.

The energies of the mesons that stopped in the detectors were determined from computed range-energy curves,[12] and the range-energy curves for glass[13] and emulsion.[14]

C. Detectors

When photons strike deuterons, both π^+ and π^- mesons are produced. In the presence of matter π^- mesons are almost invariably captured as they come to rest. π^+ mesons, on the other hand, are repulsed by the coulomb field of the nucleus and decay with a characteristic mean lifetime of 2.5×10^{-8} sec.[15] into μ^+ mesons with energies of 4 Mev.

For this experiment the characteristic endings were used to distinguish π^+ and π^- mesons in the nuclear emulsions. The π-μ coincidence detection method used by Jakobson, Schulz and Steinberger,[15b] the β^+ decay of the μ^+ meson used by several experimenters, here called π - β coincidence detection, and coincidences between these two methods, called π-μ-β detection, were chosen for the detection of the π^+ mesons. The crystal detection was used to obtain detailed statistics of the energy distributions, and the nuclear emulsions for fixing the absolute

---

12. W. A. Aron, B. G. Hoffman and F. C. Williams, UCRL-121, 2nd Rev. (1949)

13. W. A. Aron, Range-energy curve for glass, Private Communication

14. H. Bradner, F. Smith, W. Barkas and A. S. Bishop, Phys. Rev. 77, 462 (1950)

15a. C. Wiegand, Phys. Rev. 83, 1085 (1951)
b. M. Jakobson, A. Schulz and J. Steinberger, Phys. Rev. 71, 894 (1951)

cross sections and for determination of the deuterium minus-plus ratios.

1. Crystal coincidence detection. Some of the π^+ mesons which left the target passed through the absorber and first crystal and stopped in the second crystal, as illustrated in the block diagram of the electronics, Fig. 5. The individual pulses were viewed by separate photomultipliers and the signals were sent to a Wiegand-type distributed coincidence.[16] The coincidence pulse was delayed 0.025 microseconds by RG63/U cable, and was used to open a gate of 8×10^{-8} sec. duration. If the π^+ meson decayed into a μ^+ meson during the time interval that the gate was open, a delayed coincidence resulted and the meson was counted on Scaler 2. The accidental background for the $\pi-\mu$ coincidence was obtained by delaying the gate for a time long compared to the π^+ mean life. In a similar manner, the $\pi-\pi$ coincidence pulse was used to open a series of β gates. The beta delayed coincidences were registered on Scalers 7, 8, 9, and 10. As the μ^+ mean life is about 2.2×10^{-6} sec., shaping circuits were used along with the slower coincidence circuits. The first beta gate was then put into coincidence with the $\pi-\mu$ signal to form the $\pi-\mu-\beta$ coincidence, which was then registered on Scaler 11.

Different counting methods were used to count the same events; therefore, it would appear possible to determine the efficiencies of each of the three methods and the actual number of π^+ mesons that stopped in the second crystal. This determination is dependent on the fact that all, or a known fraction, of the π^+ mesons that stopped in the second crystal opened gates. No clear-cut π^+ meson plateaus were observed for the pulses from the second crystal. Therefore, instead of obtaining efficiencies in this manner, they were calculated from the nuclear

---

16. C. Wiegand, Rev. Sci. Inst. 21, 975 (1950)

emulsion data. This determination showed that at the photomultiplier voltages used, about 1200 volts, only about half of the π^+ mesons which stopped in the last crystal opened gates. The measured efficiencies and the typical ratios of the background counts to true counts are given in Table II. The counting rate for the $\pi-\mu$ coincidences was of the order of one per minute at the emission angle of 90° and meson energies of 70 Mev. The observed background counting rates were compatible with those calculated.

Table II. Crystal Coincidence Detection Efficiencies and Background

Detection Method	Efficiency	Background Counts / True Counts
$\pi-\beta$	0.27	2 - 5
$\pi-\mu$	0.077	0.10 - 0.20
$\pi-\mu-\beta$	0.027	~0.01

The following additional evidence may be presented that π^+ mesons were being detected. 1) When the maximum photon beam energy was reduced below the threshold for meson production no mesons were counted. 2) The shape of the π^+ meson energy distribution at 90° compares well with the one obtained by Bishop, et al.[2d] 3) The relative shapes of the distributions obtained by each of the counting methods agree, within statistics, at both 90° and 135°. 4) The counter data is in good agreement with the emulsion data for the relative shapes of the spectra and for the deuterium-hydrogen ratios.

A run was made with the experimental setup identical to the usual runs except with an empty pressure chamber. The meson counting rate observed was negligible compared to the normal counting rates with gas in the target.

Recently it was reported[17] that pulses in a photomultiplier were followed

17. T. N. K. Godfrey, F. B. Harrison, and J. W. Keuffel, Phys. Rev. 84, 1248 (1951)

by secondary "satellite" pulses which occurred with a definite time rate of build up and decay. The satellite pulses were counted down to one-thirtieth of the minimum main pulse size. For the delayed coincidences of this experiment, on the other hand, the A pulses required were about one-tenth of the maximum pulse that might be expected from a stopping proton.

In order to determine whether or not satellite pulses would be sufficiently large to make a delayed coincidence at the level required by this coincidence circuit, a test was made using protons from the 32 Mev linear accelerator. The pulses from protons passing through the first crystal and stopping in the second were used to open delayed gates. The proton energy loss in the second crystal was about 15 Mev. The number of satellite pulses from the second photomultiplier was found to be negligible compared to the number of mesons which would have been recorded under running conditions of this experiment for that number of gates. Furthermore no mesons were recorded when mesons could have not stopped in the second crystal, i.e. when the maximum energy of the photon beam was reduced below the meson threshold energy.

2. Nuclear emulsion detection. Ilford C-2 nuclear emulsions were selected for detectors as their sensitivity is about optimum for meson detection. They were backed by 1 x 3 x 1/16 inch glass plates and were exposed in lead boxes in stacks of five sandwiched between glass plates. This method of exposure was economical of beam time as nuclear emulsions could be pulled at different exposures and blank glass plates inserted. The exposures ranged from 1 to 5 x 10^{12} equivalent quanta. Only those emulsions which recorded the lowest energy mesons, (thin absorbers) were limited to the low exposures. The single grain background on the emulsions indicated that practically all of the background electrons were coming from the target.

In order to obtain absolute cross sections, it was necessary to have a measurement of the emulsion thickness before development. This was obtained by sending

390 Mev alpha-particles through the emulsions at an angle of 45° to the plane of the emulsion. As the emulsions shrink only in the dimension perpendicular to the plane of the emulsion, the projected track length after development is equal to the original thickness before development. The shrinkage factor obtained by this method was 2.42 ± 0.12. The relative shrinkage factors are considered to be good to 2 percent.

The method of meson identification and classification employed in this experiment have previously been reported.[2b]

The emulsion detection method is subject to several internal checks. 1) In Fig. 4 it was demonstrated that the mesons originated in the target, were collimated and scattered in the absorbers as expected. 2) From a plot of the number of meson endings, of each of the three types, versus their depth in the emulsion, the meson emulsion depth acceptance criterion was established. If the mesons end near the surface of the emulsion, or near the glass, the tracks are often shorter and therefore more difficult to identify. In addition, if prongs or mesons are emitted from the ending there is a possibility that they will be missed. Only mesons ending 3 microns or more, after development, from either surface of the emulsion were accepted. This removed about 7 percent of the available emulsion volume. 3) The projected ranges of the mesons, measured from their endings back to the point where they entered or left the emulsion were measured to about 10 percent accuracy. The similarities of the projected track length distributions for mesons with σ and π-μ endings indicated a consistent detection efficiency for both types of meson endings. The ρ distribution was compatible with a group of mesons which originated in the target superimposed on a distribution which originated in the immediate vicinity of the emulsion. The distribution of μ^+ mesons from the ends of π^+ mesons lends itself rather easily to analysis. The

expected distribution function for isotropic emission has been included along with observed distribution in Fig. 6. The curve on the plot was normalized in the region of 50 to 500 microns. As π^+ mesons with very short μ^+ meson decays are more difficult to find than those with long decay tracks or π-μ completes, the lack of μ^+ mesons in the 0-50 micron interval might be expected. The curve fitted in this manner would indicate that about 7 percent of the total π^+ mesons were not seen. It would also predict 76 π-μ completes, well within the statistics of the 80 observed. The curve was also normalized from 50 microns to infinity (all ranges above 600 microns would be included in the π-μ completes) with similar results. 4) Plots of the angular distribution of all types of mesons from deuterium for the nominal angle of 45° are shown in Fig. 7. The distribution of μ^+ mesons from the π^+ endings is uniform in angle of emission. The π^+ and π^- mesons are certainly coming from the target. The distribution of ρ endings shows a uniform background of μ^+ mesons plus a hump from the target direction. If this uniform background of μ^+ mesons and the μ^+ and μ^- mesons due to decay in flight of the π mesons are subtracted from the distribution, the remaining number of ρ endings must be from π^- mesons which do not form stars plus any μ mesons that might have been produced in the target. If all of the remaining mesons are considered to be π^- mesons which do not form stars, one arrives at the prong distribution of π^- mesons shown in Table III. The data of Adelman and Jones, Menon, and Adelman[18] has been included for comparison. If one takes their fraction of π^- mesons which do not form stars, the ratio of the cross section for μ meson production to π meson production in deuterium is -0.04 ± 0.08. Within statistics there were no μ mesons produced in the target; a similar analysis

---

18. F. L. Adelman, Phys. Rev. 85, 249 (1952)

of the hydrogen data gives the same result. This value is in agreement with the experiment in which carbon was bombarded by photons.[2b] If, on the other hand, one assumes no α mesons are made in the target, the experimental fraction of π^- mesons which give no ionizing tracks at their endings agrees within statistics with the value of Adelman and Jones.[19]

Table III. Fractional number of prongs from σ^- mesons

	from 303 σ^- mesons	Adelman and Jones, Menon et al., Adelman[18] from 3366 σ^- mesons
σ_0	0.23 ± 0.08	0.268 ± 0.021
σ_1	0.26 ± 0.03	0.237 ± 0.007
σ_2	0.28 ± 0.03	0.239 ± 0.007
σ_3	0.15 ± 0.02	0.163 ± 0.006
σ_4	0.06 ± 0.01	0.077 ± 0.004
σ_5	0.02 ± 0.01	0.014 ± 0.001
σ_6	0.003 ± 0.003	0.001 ± 0.001

Identical scanning of the same emulsion by different observers indicated that the absolute efficiencies of observers is greater than 90 percent. Analysis of the projected ranges of α^+ mesons indicated that absolute efficiencies for the observation of π^+ mesons was greater than 90 percent, but that probably some short π^+ mesons with short α^+ meson decays were missed. Some short π^- mesons

---

19. F. L. Adelman and S. B. Jones, Science 111, 226 (1950)

are slightly easier to identify than short π^+ mesons because of the heavily ionizing tracks at their endings; on the other hand, some of the short π^- mesons may be confused with the low-energy photo-induced stars in the emulsion and might not be counted. In view of these arguments it is felt that the relative detection efficiencies for π^+ and π^- mesons are about equal, and that if systematic errors are present they would tend to lower the minus-plus ratios slightly. As the absolute efficiencies are not known precisely, the data has not been corrected for observer efficiency. Individual observer error was minimized by dividing the emulsion area to be scanned into two parallel strips, each 1 cm x 2.5 cm. Each of the 2 strips was scanned by a different observer. Comparing the data from the two areas showed no systematic error that could be attributed to individual observers.

For the hydrogen exposures at each of the angles, 45° and 90°, the number of σ endings observed was less than two percent of the number of π-μ endings. All of the σ-mesons observed came from the target direction. Since photons on stainless steel should give about as many π^+ as π^- mesons, it follows that the background of π^+ or π^- mesons from the target walls is less than 2 percent of those produced in the gas. However, if all of the mesons came from the target gas, one has the result that the ratio of the number of π^- to π^+ mesons from hydrogen is about 0.02; this alternative is considered quite improbable.

The total volume of emulsion scanned for the deuterium exposures was about 0.9 cm^3, for the hydrogen exposures about 0.6 cm^3.

III. RESULTS

A. Minus-Plus Ratio for Deuterium

A quantity which should be independent of beam monitoring, density of the

bombarded gas, and geometry considerations is the ratio of the number of π^- to π^+ mesons produced. In a particular π meson energy interval and angle of emission, the minus-plus ratio is simply

$$\frac{[\pi^-]}{[\pi^+]} = \frac{1.37\,[\sigma]}{[\pi-\mu]}$$

where $[\sigma]$, and $[\pi-\mu]$ are the numbers of σ and $\pi-\mu$ meson endings found in the volume of emulsion corresponding to the particular π meson energy and angle of emission.

An alternate, less reliable, method of obtaining the ratio is of interest in indicating experimental consistency. The value of the ratio is

$$\left(\frac{[\pi^-]}{[\pi^+]}\right)_{Alt.} = \frac{2+f_d}{\dfrac{0.73\,[T]}{[\sigma]} - (1+f_d)}$$

where $[T]$ is the total number of meson endings of all types observed, and f_d is the fraction of π mesons which decay in flight before reaching the detectors. This method is considered less reliable because a count of the total number of mesons includes ρ endings which are more difficult to identify than either σ or $\pi-\mu$ endings as there is no distinguishing event at their endings.

The values for the minus-plus ratios from deuterium are given in Table IV.

TABLE IV MINUS-PLUS RATIO OF π MESONS FROM DEUTERIUM

Angle $\bar{\theta}$	E (Mev)	Ratio	Ratio (Alternate Method)
45°	43	0.79 ± 0.21	0.75 ± 0.22
	57	1.04 ± 0.16	1.15 ± 0.21
	87	0.89 ± 0.21	0.91 ± 0.24
	128	0.99 ± 0.30	0.73 ± 0.26
45° (Mean)		0.96 ± 0.10	0.94 ± 0.13
90°	34	1.24 ± 0.20	1.38 ± 0.32
	70	0.98 ± 0.14	1.08 ± 0.19
90° (Mean)		1.09 ± 0.12	1.20 ± 0.17
135°	39	1.37 ± 0.22	1.06 ± 0.20
	57	1.05 ± 0.18	1.13 ± 0.26
135° (Mean)		1.21 ± 0.17	1.08 ± 0.16
All Angles (Mean)		1.07 ± 0.07	1.04 ± 0.09

It is interesting to note that these ratios are close to one, and are independent of energy or angle, within statistics, for the energies and angles investigated. A ratio of one is in agreement with the value of Littauer and Walker[2g], who found, for the emission angle of 135° and a π^+ meson energy of about 50 Mev, a minus-plus ratio of 1.19 ± 0.12. Further evidence of this independence was furnished by Lebow et al.[2k], who found ratios of 0.5 ± 0.5 and 0.30 ± 0.23 at 90° and 26°, respectively.

Theoretical calculations of the minus-plus ratios have been carried out.[20,5b] If the interaction of the photon with the currents due to moving charges, only, is considered, the resulting minus-plus ratio varies with the meson energy and angle of emission and is considerably greater than one for high energy mesons.

Better agreement with the experimental results is obtained if the interaction is primarily through the static magnetic moments of the nucleons. This gives a minus-plus ratio which is essentially independent of the angle of emission or the energy of the meson.

B. Cross Sections for Hydrogen and Deuterium.

For a line source emitting π mesons, in the case where there are only two particles in the final state, e.g., photons bombarding protons to give a meson and a neutron, as shown in Fig. 8, the differential cross section can be found from the following formula:

---

20. K. A. Brueckner and M. L. Goldberger, Phys. Rev. 76, 1725 (1949)
K. A. Brueckner, Phys. Rev. 79, 641 (1950)
G. Araki, Progress of Theoretical Physics 5, 507 (1950)

$$\frac{d\sigma(\bar{\theta},k)}{d\omega} = \frac{1}{\epsilon} \frac{\Delta N}{hd\, G(\bar{\theta}) \left(\frac{dq}{dk_o}\right) \left(\frac{dk_o}{dE}\right) \left(\frac{dE}{dR}\right) n}$$

where ϵ is the efficiency of the detector.

h is the effective neight of the detector.

w is the effective width of the detector.

d is the effective length of the detector.

ΔN are the number of counts observed at a particular meson energy E, and average angle of emission, $\bar{\theta}$.

dq/dk_o are the number of quanta of energy k per unit energy, which contribute to the production of the mesons. This factor depends on the detailed shape of the bremsstrahlung spectrum.

dk_o/dE relates the photon energy interval to the meson energy interval. This factor may be obtained from knowledge of $k_o = f\ (E,\bar{\theta})$

dE/dR relates the range interval of the detector to the energy interval of mesons leaving the target. It is a function of $\bar{\theta}$ and E.

n is the number of target praticles per unit volume, in this experiment, either the number of protons or neutrons per unit volume.

$G(\bar{\theta}) = \iint \frac{dwdt}{R^2} = \frac{1}{a} \iint dwd\theta$ This is the geometrical factor that changes only in going from one average angle to another.

R is the distance from an interval of length of the target, dt, to the detector.

a is the perpendicular distance from the line source to the detector.

If there are more than two particles in the final state, the energy of the π meson is not a single valued function of the photon energy, and dk/dE is not defined. One method of evaluating data is to replace $\frac{dq}{dk}dk$ by the number of equivalent quanta, Q, where the number of equivalent quanta is defined as the total energy in the beam divided by the maximum photon energy. The cross section, with the number of equivalent quanta defined in this way is then

$$\frac{d^2\sigma(\bar{\theta},E)}{dE\, d\Omega} = \frac{\Delta N}{\epsilon\, hd\, G(\bar{\theta})\, Q\left(\frac{dE}{dR}\right)_n}$$

The differential cross section, $\frac{d\sigma(\bar{\theta})}{d\Omega}$, can be found by integrating $\frac{d^2\sigma(\bar{\theta},E)}{dE\, d\Omega}$ over dE and the total cross section by integrating the differential cross section over the solid angle. The data was extrapolated from 0 to 40 Mev to obtain the differential cross sections, and over the angles that were not measured to obtain the total cross sections.

In order to obtain the cross sections, certain corrections were applied to the data. These corrections were: 1) Decay in flight of the π mesons. A value for the mean life of the π meson was taken to be 2.5×10^{-8} sec.[15]. This correction is small, varying from 5 percent at low meson energies to 2.5 percent at high. 2) Slit penetration. The geometry factor, $G(\bar{\theta})$, was calculated on the basis of perfectly opaque slits to the π mesons. This is obviously an over simplification as some mesons of high energy may penetrate the slit and still have enough energy to reach the detectors; these mesons will then be observed at a lower meson energy. The correction was made by calculating the increase in slit width, and thus the geometrical factor, as a function of the meson energy. 3) Multiple scatter. For the emulsion detection the condition for "poor geometry" was satisfied. The front edge of the emulsion was in contact with the lead

absorber. The thickness of the emulsion, about 2×10^{-2} cm, was very small compared to the height of the lead absorber, 4.5 cm, and the absorber and meson beam were wide compared to the width of the emulsion scanned. The r.m.s. displacements for mesons traversing the lead and glass absorbers were calculated using methods which consider energy loss of the mesons[11], and the net loss of π mesons to the emulsion detectors was found to be negligible. In the case of crystal detection the poor geometry condition was not entirely satisfied because of the large size of the crystals and their position with respect to the absorbers. The resulting correction factors, which have been applied to all subsequent data, are shown in Fig. 9.

A fourth correction is for nuclear interactions in the absorbers. Because some mesons may be absorbed, or undergo large angle scattering in interacting with nuclei, they will not reach the detector. The evidence, at the present time, indicates that the cross section for nuclear events for π mesons in flight traversing matter is of the order of a geometrical nuclear area.[21] The values of nuclear areas found from high energy neutron scattering experiments were used in obtaining these correction factors.[22] This correction varies from about 8 percent at a π meson energy of 35 Mev to 85 percent at 150 Mev.

1. Energy Distributions in the Lab System. The energy distributions for π^+ mesons with the appropriate corrections have been calculated per equivalent quantum, Q, and are plotted in Fig. 10 for each of the production angles, 45°, 90°, and 135°. The crystal data which was obtained by the three detection

---

21. C. Chedester, P. Isaacs, A. Sachs, and J. Steinberger Phys. Rev. 82, 958 (1951)

22. L. Cook, E. McMillan, J. Peterson and D. Sewell, Phys. Rev. 75, 7 (1949) S. Fernbach, R. Serber and T. B. Taylor, Phys. Rev. 75, 1352 (1949)

methods $\pi-\iota$, $\pi-\beta$ and $\beta-\mu-\beta$ have been combined. The energy distribution for π^- mesons from deuterium is also plotted at 45°. The absolute cross section scale for the crystal data was fixed by the emulsion data from hydrogen and deuterium at the emission angle of 90° and meson energy of 70 Mev. The relative values of the hydrogen to deuterium energy distributions, as obtained by the crystal detection, were not altered by this emulsion normalization. The agreement between crystal and emulsion data at other points is good.

Smooth curves have been drawn through the data and extrapolated to zero meson energy for the purpose of integration. The dashed curves have been corrected for nuclear interaction. The tails on the energy distributions, which appear at meson energies above that allowed by conservation of energy and momentum at the angles, $\bar{\theta}$, are due to those mesons which are allowed through the collimating system at angles smaller than $\bar{\theta}$. The shape of the hydrogen spectrum at 90° compares favorably with that of Bishop et al.[2d] when the tail is taken into account. The absolute value of the peak of the hydrogen spectrum is in agreement with the recently renormalized value of Steinberger and Bishop[2e]--hereafter referred to as S.B. From Fig. 10 it is seen that the distributions for hydrogen and deuterium are similar in shape.

The uncertainties in Fig. 10 and in subsequent curves are standard deviations due to statistics only. The relative photon beam integration for the experiment is considered to be as good as 2 percent. The values at 45° relative to those at 90° and 135° are only as good as the normalization of the plate data, about 10 percent. The largest uncertainty in absolute values is that of the absolute beam integration which may be as large as 20 percent.

2. Differential Cross Sections per Q in the Lab System. The differential cross sections for π^+ mesons were found by integrating under the curves of Fig. 10; they are plotted in Fig. 11. The values could be changed somewhat by a different extrapolation to zero meson energy. Smooth curves have been drawn through the data for the purpose of obtaining total cross sections. The dashed curves have been corrected for nuclear interaction.

3. Total Cross Sections per Q. The total cross sections for π^+ mesons from hydrogen and deuterium per Q were found by integrating the differential cross sections of Fig. 11 over the solid angle. In addition to the uncertainties listed previously there is the uncertainty due to the extrapolation over angles for which the differential cross sections were not obtained. Since the solid angle approached zero at 0° and 180°, this introduces a small error.

The total cross sections are given in Table V. The uncertainties in Table V are those of the absolute beam integration.

Table V. Total Cross Sections per Q for π^+ Mesons from Deuterium and Hydrogen

Target	σ_T cm^2 Q^{-1} proton^{-1}	σ_T corrected for nuclear interaction
deuterium	$6.4 \pm 1.3 \times 10^{-29}$	$7.7 \pm 1.5 \times 10^{-29}$
hydrogen	8.3 ± 1.7	10.3 ± 2.1

4. Deuterium-hydrogen ratios for π^+ meson production. The ratios of the cross sections for the production of π^+ mesons from deuterium and hydrogen, as obtained from the energy distributions for several energies at each of the production angles, are plotted in Fig. 12. These ratios are dependent only on the relative beam monitoring, and in the case of emulsions, also on the relative plate thickness. Therefore, the largest uncertainties are given by the statistics.

Chew and Lewis[4a,b] and others[5] have used an interaction of the form $L + \sigma \cdot K$ and the impulse approximation to theoretically investigate this deuterium-hydrogen ratio. They point out that in order to calculate the ratio, it is necessary to evaluate certain overlap integrals over the relative momentum of the two outgoing neutrons using the initial deuteron and final di-neutron wave functions. If these functions are known, the calculation is possible. For the initial deuteron wave function, four authors[4a,4b,5b,5c] have used the Hulthen wave function

$$\psi_D = \sqrt{\frac{\alpha\beta(\alpha+\beta)}{2\pi(\beta-\alpha)^2}} \quad \frac{e^{-\alpha r} - e^{-\beta r}}{r}$$

and one[5a] has used the above with $\beta = \infty$. From the low energy (n,p) scattering cross section, and the coherent scattering amplitude of neutrons scattered from hydrogen[23,24], the value of the effective range, and thus β can be obtained. The neutrons in the final state have been treated as plane waves[4b,5a,5c] as ending in a ^1S state[5b,5c], and closure theorems have been invoked to perform the integrations over the final state.[4a] The plane wave treatment neglects the interaction between the two neutrons which occurs when their relative momentum is small. The ^1S state treatment is only valid for low relative momentum between the two nucleons, and the closure method sums over all values of the relative momentum, some of which are not allowed by conservation of energy and momentum, and thus tends to overestimate the ratio.

Chew and Lewis[4a] give the deuterium-hydrogen ratio in the form

$$\left[\frac{\left(\frac{d\sigma}{d\Omega}\right)_D}{\left(\frac{d\sigma}{d\Omega}\right)_H}\right]_{k_o} = \left[1 - \frac{q_o^o}{M}\left(1 - \frac{k_o^o \cos\theta}{q^o}\right)\right] \int_{m_q}^{q_o^{max}} \frac{q_o q}{q_o^o q^o} \left[\frac{L^2(F_1-F_2) + K^2\left(F_1 - \frac{F_2}{3}\right)}{L^2 + K^2}\right] dq_o$$

23. J. M. Blatt and J. D. Jackson, Phys. Rev. 76, 18 (1949)

24. D. J. Hughes, M. T. Burgy, and G. R. Ringo, Phys. Rev. 77, 291 (1950)

where M is the proton rest mass, q_o, q, and m_q are the meson total energy, momentum, and rest mass, respectively, in units of Mev. F_1 and F_2* are functions of ϑ, k_o, and q_o where θ is the meson angle with the beam direction and k_o is the photon energy. A super c, i.e., q^c, refers to the kinematics for the free nucleon case. The data has been compared to the theoretical predictions obtained by two different methods.

Method 1: The above indicated numerical integration is evaluated for a given k_o. It has been previously pointed out that there is no unique relationship among ϑ, k_o, and q_o for mesons produced from deuterons, as is the case for mesons from protons. If the assumption is made that the deuterium meson energy spectrum from a given k_o is narrow and that the peak occurs at the line spectrum from hydrogen, other photons will not contribute appreciably to the number of mesons at a particular θ, and meson kinetic energy, E. The experimental ratio at a given meson kinetic energy can be then compared to the theoretical ratio for a photon energy obtained by the free particle kinematics. In Fig. 12 are plotted the dotted curves obtained in this manner. Those marked $K^2/L^2 = \infty$ refer to all spin interaction, and those marked $K^2/L^2 = 0$, to no spin interaction. These curves have been evaluated for the Hulthén deuteron function for $\beta = 6a$. The experimental effective range[24] of 1.71×10^{-13} cm fixes the value of β to within a few percent. It can be seen from the dotted curves that the theoretical

---

*The F_1 and F_2 of Chew and Lewis[4a] are related to the F- and F+ of Saito et al.[5c]

by $F_- = \frac{q}{2k_oA^2}(F_1 - F_2)$ and

$$F_+ = \frac{q}{2k_oA^2}\left\{F_1 + F_2 + \frac{4}{\beta^2 - a^2} \ln \left[\frac{(n+1)^2 + a^2}{(n-1)^2 + a^2} \quad \frac{(n-1)^2 + \beta^2}{(n+1)^2 + \beta^2}\right]\right\}$$

where $A^2 = \sqrt{\frac{a\beta(a+\beta)}{2\pi(\beta - a)^2}}$, $\vec{1} = \frac{\vec{n_1} + \vec{n_2}}{2}$, $\vec{n} = \frac{\vec{n_1} - \vec{n_2}}{2}$, and $\vec{n_1}$ and $\vec{n_2}$ are the momenta of the two resultant neutrons.

deuterium-hydrogen ratios are less than one and increase with increasing meson energies (photon energies). The data, on the other hand, have a distinct downward trend at each of the angles. This disagreement is a direct consequence of the neglect in the theoretical ratio of the contribution of mesons from other photons in the bremsstrahlung to the detected energy interval. The assumption of a narrow spectrum is only valid for meson angles near 0^o.

Method 2: If the assumption is made that the spin flip probability, $K^2/(K^2 + L^2)$ is not strongly dependent on the photon energy, the theory can be evaluated for the experimentally determined quantity $\left(\frac{d^2\sigma}{dEd\Omega}\right)_D \left(\frac{d^2\sigma}{dEd\Omega}\right)_H$. This is done by performing the integration over the bremsstrahlung spectrum at a fixed meson energy. The resulting ratio is then given by

$$\frac{\left(\frac{d^2\sigma}{dEd\Omega}\right)_D}{\left(\frac{d^2\sigma}{dEd\Omega}\right)_H} = \frac{\left[1 - \frac{(k^o - q^o \cos\theta)}{M}\right]}{\mathcal{B}(k_o^o)\,\mathcal{E}(k_o^o)} \int_{q_o min}^{q_o max} \frac{\left[L^2(F_1 - F_2) + K^2(F_1 - F_{2/3})\right]}{(L^2 + K^2)} \mathcal{B}(k_o)\mathcal{E}(K_o)\,dk_o$$

where $\mathcal{B}(k_o)$ is the bremsstrahlung photon energy distribution from a 20 mil platinum target corrected for the spread-out beam with an upper limit photon energy of 322 Mev. k^o is the photon momentum and $\mathcal{E}(k_o)$ is the excitation function for π^+ mesons from hydrogen. The excitation functions used in the numerical integration of this ratio were those of Steinberger and Bishop[2e], Feld et al.[2j] and of this paper (see the section on excitation functions) for the angles of 90, 26, and 135 and 45 degrees, respectively. The computed ratio is not very sensitive to the excitation functions used. From the solid curves obtained in this manner it is seen that the theoretical ratio drops rapidly near the upper end of the bremsstrahlung and is equal to zero at maximum photon energy. This drop-off is due to the effect of the cut off of the photon spectrum and the broad meson spectrum from deuterium for monoenergetic photons.

The solid curves fit the data very well at 90 and 45 deg. but drop off too sharply at 135 deg. This departure can be mainly attributed to the effect of the angular uncertainty of ± 19 deg. in the experimental data. Mesons contributed to the detector from smaller angles tend to increase the ratio which is measured at a given meson energy. The change in meson energy with angle at a fixed photon energy is much more rapid in the backward directions, thus the angle uncertainty has more effect at 135 than at 90 and 45 deg. In addition an uncertainty in the theoretical deuterium meson energy distributions would give the greatest uncertainty in the ratio near the cut-off of the bremsstrahlung.

At each of the angles, the deuterium-hydrogen ratios were averaged over the energy intervals where data exist and are given in Table VI. The theoretical values obtained in the same manner are also given. The values of Lebow et al.[2k] at 26 and 90 deg. have been included.

The agreement between experiment and theory gives strong support for the validity of the impulse approximation. From Fig. 12 and Table VI it can be seen that the statistics of the data are not sufficient to determine the fraction of spin interaction. In order to have a large exclusion effect, and thus large differences in the ratios for all and no spin interaction the relative momentum between the two outgoing neutrons must be small.[3,4] Unfortunately this occurs at small angles to the photon beam direction where the background due to electrons is very high. At these forward angles where the exclusion effect is large, the deuterium spectrum is also sharp and the bremsstrahlung spectrum does not present a problem.

It should be kept in mind that the theoretical ratios are dependent on the initial deuteron and final nucleon wave functions. Computations have been carried out for the case of the Hulthén deuteron wave function in the initial state with $\beta = \infty$, and for plane waves for the nucleons in the final state. The

Table VI. Deuterium-hydrogen ratios, $\left(\frac{d^2\sigma}{dE\,d\Omega}\right)_D \Big/ \left(\frac{d^2\sigma}{dE\,d\Omega}\right)_H = \frac{D}{H}$, averaged over the meson kinetic energy interval, ΔE, where data exists.

θ (deg)	ΔE (Mev)	Δk_o (Mev) (b)	$\overline{\left[\frac{D}{H}\right]}$ Exp	$\overline{\left[\frac{D}{H}\right]}$ Theory 1 (c)		$\overline{\left[\frac{D}{H}\right]}$ Theory 2 (d)	
				$K^2/L^2 = \infty$	$K^2/L^2 = 0$	$K^2/L^2 = \infty$	$K^2/L^2 = 0$
26	65-145	212-296	0.89±0.17 (a)	0.72	0.41	0.71	0.41
45	38-134	190-300	0.74±0.08	0.76	0.57	0.84	0.63
90	40-105 39-93	212-322 210-300	0.64±0.18 (a) 0.74±0.05	0.81	0.73	0.80	0.72
135	37-67	230-300	0.79±0.06	0.82	0.77	0.71	0.64

(a) Data of Lebow et al.[2k]

(b) Photon energy interval from free particle kinematics corresponding to ΔE.

(c) Computed by Method 1.

(d) Computed by Method 2.

values obtained for the ratio were much lower than the curves of Fig. 12. On the other hand, computations using the Hulthén function with $\beta = 6\alpha$ and closure in the final state give ratios slightly larger than the curves of Fig. 12.

The experimental value of the ratio of the total cross sections is 0.75 ± 0.04. In this case the value is dependent on the relative shapes of the energy spectra at angles which were not measured. Systematic errors due to this could cause uncertainties larger than the statistical uncertainties.

5. Excitation Functions for Hydrogen and Deuterium in the Lab System

The excitation function for π^+ mesons from hydrogen per photon of energy, k_γ has been computed. For the case of deuterium, one can make the assumption of the previous section to calculate dk/dE from hydrogen kinematics to get an excitation function for deuterium. Again, this approximation is good only at small meson angles. The excitation functions, so calculated, appear in Fig. 13. The data has been corrected for nuclear interaction. In order to improve the statistics, the π^+ and π^- mesons from deuterium have been combined; a minus-plus ratio of one was taken. The data have been fitted to straight lines, so that it could be used to find points on the angular distribution in the center of mass system. The excitation function found by S.B.[2e] has been superimposed for the purpose of comparison.

It should be pointed out that this experiment is primarily a survey experiment to compare the deuterium and hydrogen productions and was not designed

to investigate the excitation function, or the angular distribution in the manner of the previous experimenters.[2e] Although quite inconclusive, the excitation function for hydrogen of this experiment is consistent with that of S.B. for the production angle of 90°. The excitation curves for deuterium show similar trends with somewhat better statistics.

6. Differential Cross Sections for Hydrogen and Deuterium in the Center of Mass System. Points on the angular distribution curves, for various photon energies were obtained by cutting through the excitation function curves at different photon energies. The angles and cross sections were transformed to the center of mass system and are plotted in Fig. 14. The angular distribution of S.B. is included for comparison. Three points on an angular distribution curve are obviously not sufficient to determine its shape. The agreement between the data of Fig. 14 for 255 Mev photons on hydrogen and the S.B. data is good. Both sets of data tend to show the apparent peaking at an angle larger than 90° in the center of mass system. The curves for other photon energies are drawn only to show a possible trend of the angular distributions as a function of the photon energy.

The theoretical implications of the excitation curves and angular distributions for hydrogen have been treated by S.B. and by G. Araki[25].

IV. CONCLUSIONS

In summary, one can draw the following conclusions from this experiment: 1) The minus-plus ratio for deuterium is close to one, and within statistics, independent of the production angle or energy of the π meson. This implies

---

25. G. Araki, Phys. Rev. 82, 959 (1951)

a production interaction which is primarily through the magnetic moments of the nucleons, and independent of the charge carried by the nucleon except to determine the charge of the π meson produced.

2) The experimental ratios of the deuterium to hydrogen cross-sections are in agreement with the phenomenological theory of Chew and Lewis when the theory is treated in the following way: a) The Hulthén potential with $\beta = 6\alpha$ is used in the initial state; b) Plane waves are used for the nucleons in the final state; and c) The bremsstrahlung cut-off is taken into account (Method 2). This agreement gives strong support to the validity of the impulse approximation.

Computations using $\beta = \infty$ in the initial state and plane waves in the final state give values for the ratio much lower than the experiment. Computations using $\beta = 6\alpha$ in the initial state and closure in the final state give values slightly higher than the experiment. The treatment of the theory by Method 1 does not give the observed variation of the ratio with meson energy. This method will only be good at small angles to the beam where the meson distribution from deuterium becomes extremely narrow so that the bremsstrahlung spectrum may be neglected.

The statistics of the experiment are not sufficient to determine the amount of spin interaction.

3) The excitation function for hydrogen is consistent with that of S.B. for the production angle of 90°. The excitation curves for deuterium show trends which are similar to those for hydrogen. The points on the angular distribution for π^+ mesons from hydrogen in the center of mass system for a photon of 255 Mev are in agreement with the curve of S.B. with the apparent peaking at an angle larger than 90°. The points from deuterium show similar results to those from hydrogen.

It has been strongly emphasized by Chew and Lewis[4a,4b] and others that measurements of the spin flip probability for π^+ meson production from deuterium should be carried out at small angles to the beam direction. Here the exclusion effect is much greater, the assumptions of the theory are better, and the comparison between theory and experiment is more exact. Present investigations are being carried out along these lines.

ACKNOWLEDGMENTS

We wish to express our appreciation to Professor E. M. McMillan for his continued guidance and support. We would like to thank Professors W. K. H. Panofsky and O. Chamberlain and Dr. R. Lelevier for much helpful discussion. We are indebted to Dr. R. L. Aamodt and Professor W. K. H. Panofsky for the use of the deuterium pumping system, to Professors G. F. Chew and H. W. Lewis for unpublished calculations on photomeson production from deuterons. We wish to thank Mr. Collin Moore and Mr. Evan Bailey for help with the emulsions, Mr. J. A. Winokur and Robert L. Pexton for numerical computation, and Dr. W. H. Barkas and other members of the Film Group for the use of their facilities. Our sincere thanks go to Mr. George McFarland and members of the synchrotron crew for help in making the bombardments.

FIGURE CAPTIONS

Fig. 1 Schematic layout of the essential experimental components.

Fig. 2 Section through the gas target assembly.

Fig. 3 Schematic drawing of vertical and horizontal sections through the gas target and the collimating system with the detectors in position.

Fig. 4 Plot of the angular distribution of π^+ and μ^+ mesons for the 45° and 90° collimating systems demonstrating the angular resolution. The data was obtained from the emulsions. The mesons had a mean initial energy of 70 Mev and a final energy of 2 Mev; the angles were measured at 200 microns back from the meson endings. The dotted line represents the calculated angular resolution neglecting multiple scattering. This channel resolution was folded into the multiple scattering of the mesons in passing through the absorbers to obtain the solid smooth curve.

Fig. 5 Block diagram of the electronics used in the crystal coincidence detection.

Fig. 6 Projected track length distribution of μ^+ mesons. The track lengths were measured from their endings, back to the point where they entered or left the emulsion to about 10 percent accuracy. The curve on the μ^+ meson range distribution plot is the expected distribution based on normalization between 50 and 500 micron ranges.

Fig. 7 Distribution in angle of the π^--μ, ρ and μ^+ mesons from deuterium for the 45° collimating system. The angles of the tracks were measured at the point where they entered the emulsion, or 200 microns back from their ending, whichever was the shorter. The abscissa is the angle to the beam direction.

Fig. 8 Schematic drawing of the line source and detector element.

Fig. 9 Curves showing the correction factors applied to the data for time of flight, slit penetration, and multiple scattering. These are given for the coincidence crystal detection at 90° and 135°, and for the emulsion detection at 45° and 90°. No correction for multiple scattering was necessary in the case of emulsion detection.

Fig. 10 Energy distributions in the lab system at 45°, 90°, and 135° for π^+ mesons from deuterium and hydrogen and at 45° for π^- mesons from deuterium. The crystal data obtained by the 3 detection methods have been combined. Smooth curves have been drawn through the data and extrapolated to zero for the purpose of integration. The dashed curves have been corrected for nuclear interaction in the absorbers. Uncertainties shown are standard deviations due to statistics only. The horizontal lines are the detector energy widths.

Fig. 11 Differential cross sections per Q in the lab system for π^+ mesons from deuterium and hydrogen. Smooth curves were drawn for the purpose of integration and extrapolated into 0° and 180°. The dashed curves have been corrected for nuclear interaction in the absorbers. Uncertainties are standard deviations due to statistics only. The horizontal lines are the detector angular widths.

Fig. 12 Deuterium-hydrogen ratios for π^+ meson production at 45°, 90°, and 135°. The uncertainties are standard deviations due to statistics only. The horizontal lines are the energy widths of the detectors. The curves marked $K^2/L^2 = \infty$ and $K^2/L^2 = 0$ are the theoretical predictions for all spin interaction and no spin interaction, respectively. In the theoretical computations the Hulthén wave function with $\beta = 6\alpha$ has been used for the initial deuteron state and plane waves have been used for the nucleons in the final state. Method 1 and Method 2 refer to the way the theory has been compared to the data.

Fig. 13 Excitation functions for hydrogen and deuterium in the lab system. In the case of deuterium, the photon energy was assigned on the assumption that the proton was free. The data has been fitted to straight lines at each of the angles, 45°, 90°, and 135° for the purpose of obtaining points on the differential cross section curves in the center of mass system. The excitation function of Steinberger and Bishop[2e] for π^{+} mesons from hydrogen obtained from their data for an emission angle of 90° has been included for comparison. In order to improve the statistics, in the case of deuterium, the π^{+} and π^{-} mesons have been combined; a minus-plus ratio of one was taken. The data have been corrected for nuclear interaction in the absorbers. The uncertainties are standard deviations due to statistics, only.

Fig. 14 Differential cross sections for hydrogen and deuterium in the center of mass system. Curves have been drawn in to show a possible trend of the angular distribution with the photon energy. Included is the curve of Steinberger and Bishop[2e] for π^{+} mesons from 255 Mev photons on hydrogen. The uncertainties are standard deviations due to statistics only. The data have been corrected for nuclear interaction in the absorbers.

Information Division
3/31/52 bw

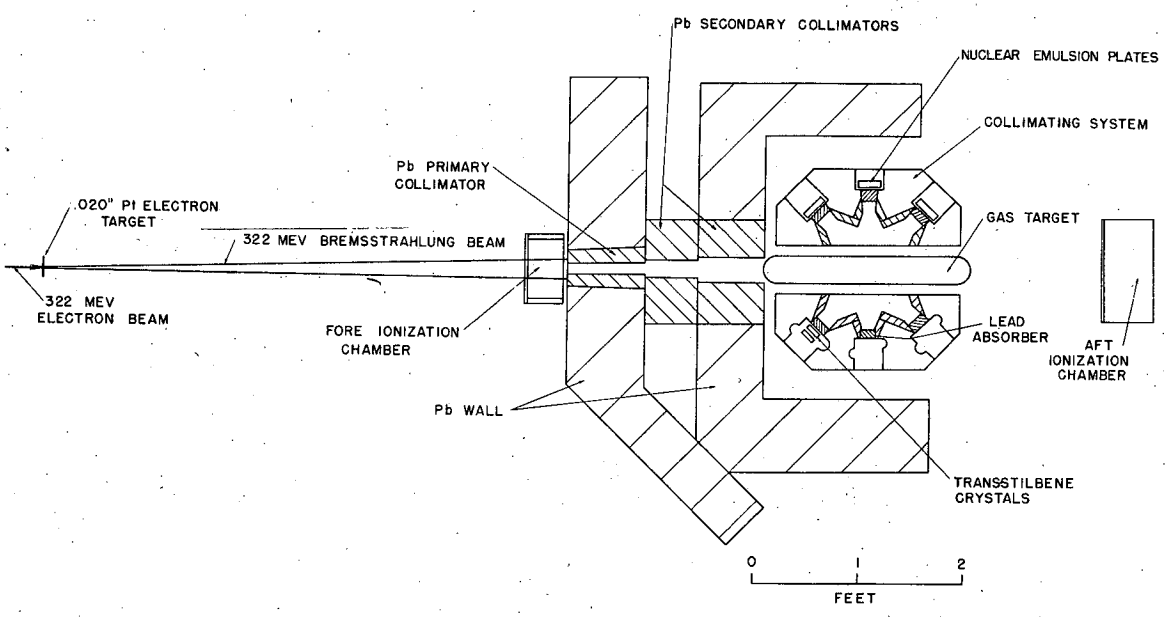
Pb SECONDARY COLLIMATORS
NUCLEAR EMULSION PLATES
COLLIMATING SYSTEM
Pb PRIMARY COLLIMATOR
.020" Pt ELECTRON TARGET
322 MEV BREMSSTRAHLUNG BEAM
GAS TARGET
322 MEV ELECTRON BEAM
FORE IONIZATION CHAMBER
LEAD ABSORBER
AFT IONIZATION CHAMBER
Pb WALL
TRANSSTILBENE CRYSTALS
0
1
2
FEET

Fig. 1

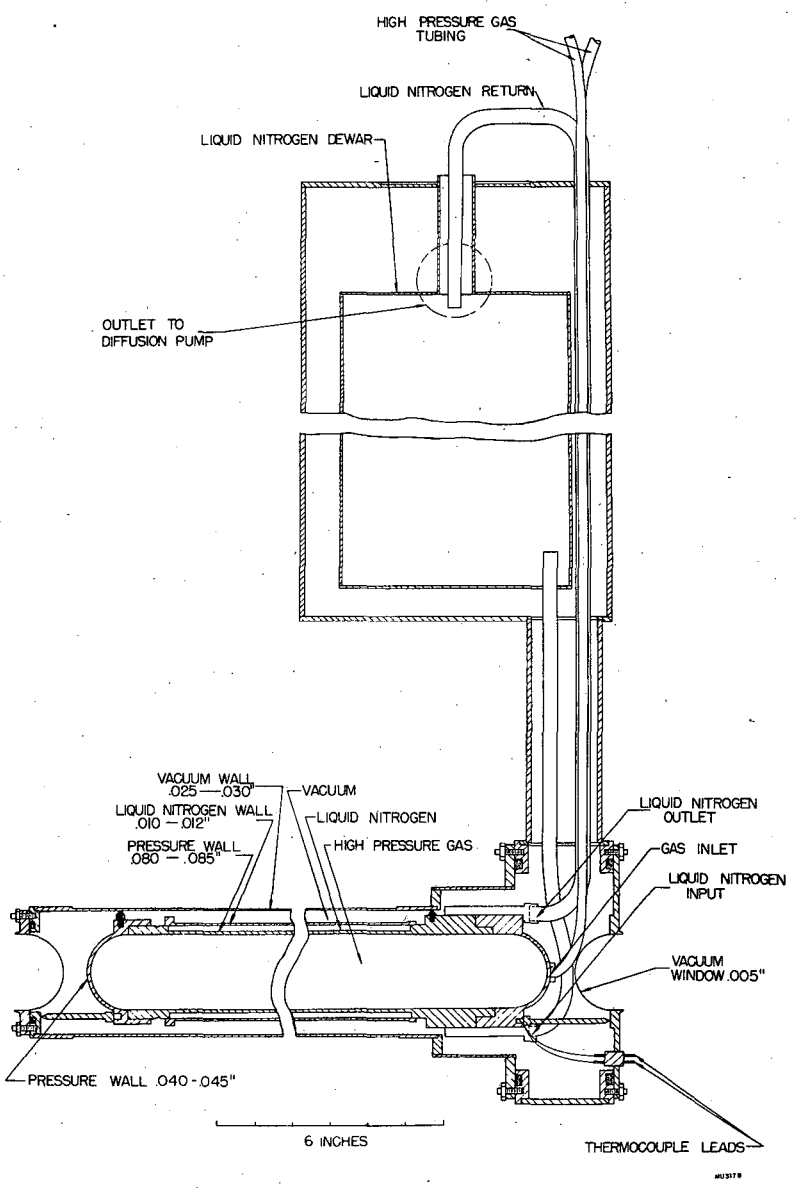
HIGH PRESSURE GAS TUBING
LIQUID NITROGEN RETURN
LIQUID NITROGEN DEWAR
OUTLET TO DIFFUSION PUMP
VACUUM WALL .025 — .030"
LIQUID NITROGEN WALL .010 — .012"
PRESSURE WALL .080 — .085"
VACUUM
LIQUID NITROGEN
HIGH PRESSURE GAS
LIQUID NITROGEN OUTLET
GAS INLET
LIQUID NITROGEN INPUT
VACUUM WINDOW .005"
PRESSURE WALL .040 - .045"
6 INCHES
THERMOCOUPLE LEADS

Fig. 2

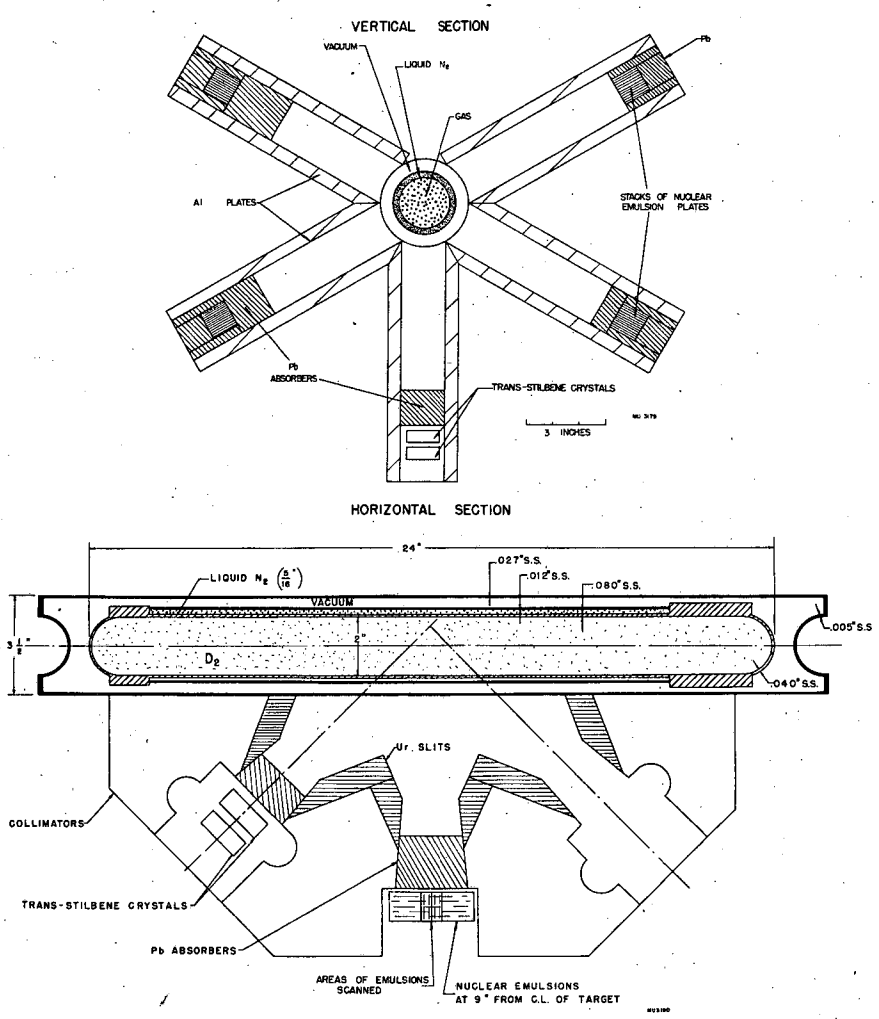
VERTICAL SECTION
VACUUM
LIQUID N_2
GAS
Pb
Al PLATES
STACKS OF NUCLEAR EMULSION PLATES
Pb ABSORBERS
TRANS-STILBENE CRYSTALS
3 INCHES
HORIZONTAL SECTION
24"
.027"S.S.
.012"S.S.
.080"S.S.
LIQUID N_2 ($\frac{5}{16}$")
VACUUM
.005"S.S
3 1/8"
2"
D_2
.040"S.S.
Ur. SLITS
COLLIMATORS
TRANS-STILBENE CRYSTALS
Pb ABSORBERS
AREAS OF EMULSIONS SCANNED
NUCLEAR EMULSIONS AT 9° FROM C.L. OF TARGET

Fig. 3

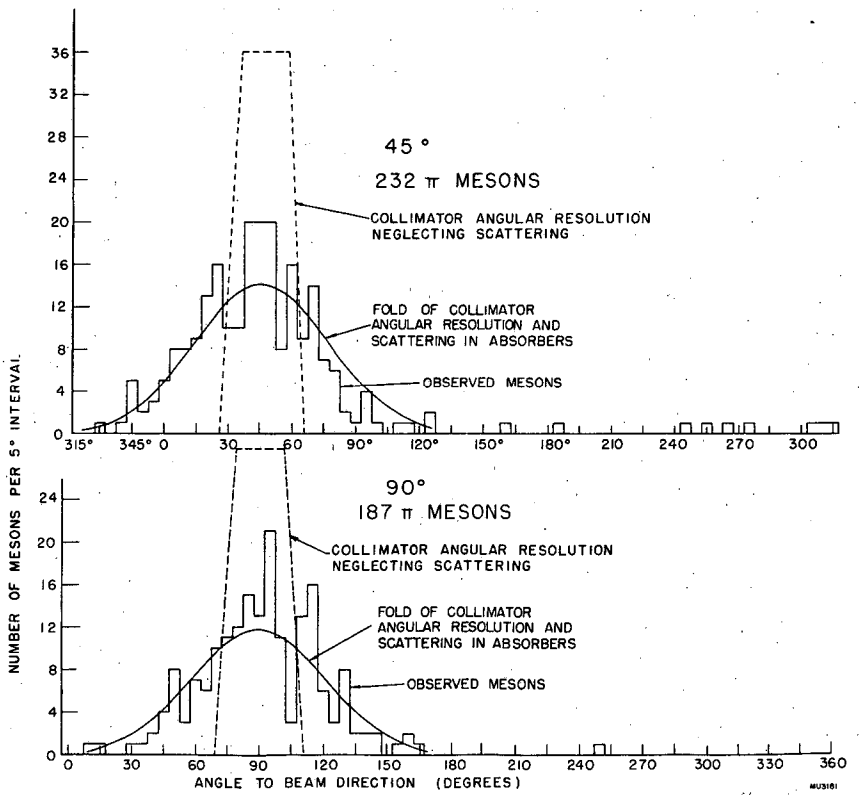
45°
232 π MESONS
COLLIMATOR ANGULAR RESOLUTION NEGLECTING SCATTERING
FOLD OF COLLIMATOR ANGULAR RESOLUTION AND SCATTERING IN ABSORBERS
OBSERVED MESONS
90°
187 π MESONS
COLLIMATOR ANGULAR RESOLUTION NEGLECTING SCATTERING
FOLD OF COLLIMATOR ANGULAR RESOLUTION AND SCATTERING IN ABSORBERS
OBSERVED MESONS
NUMBER OF MESONS PER 5° INTERVAL
ANGLE TO BEAM DIRECTION (DEGREES)
MU3161

Fig. 4

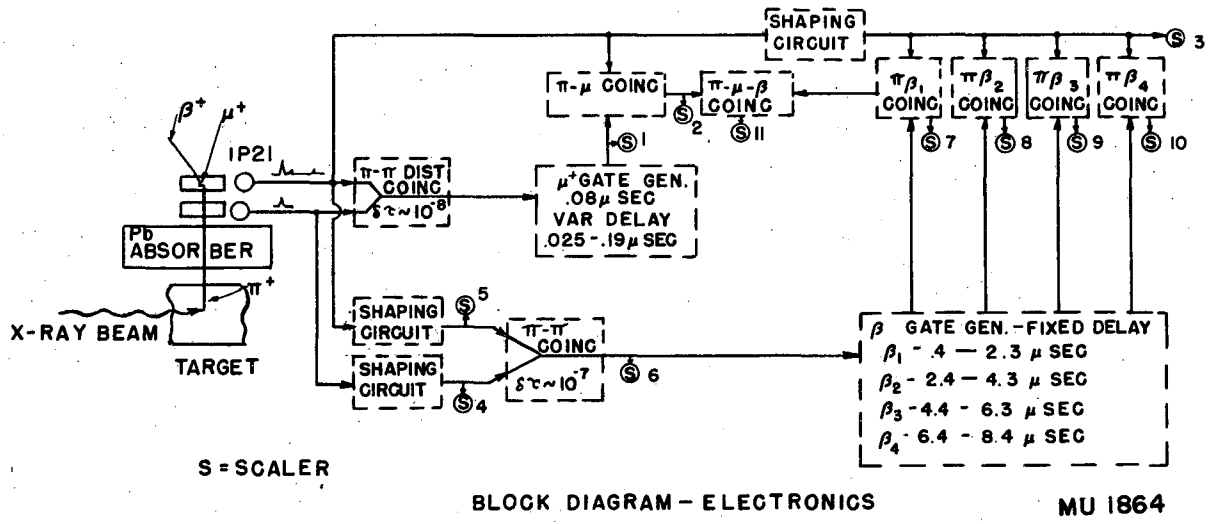
SHAPING CIRCUIT
S 3
π-μ COINC
π-μ-β COINC
πβ1 COINC
πβ2 COINC
πβ3 COINC
πβ4 COINC
S 2
S 11
S 1
S 7
S 8
S 9
S 10
β+ μ+
IP21
π-π DIST COINC
δτ~10-8
μ+GATE GEN. .08μ SEC VAR DELAY .025-.19μ SEC
Pb ABSORBER
π+
X-RAY BEAM
TARGET
SHAPING CIRCUIT
S 5
SHAPING CIRCUIT
S 4
π-π COINC
δτ~10-7
S 6
β GATE GEN.-FIXED DELAY
β1 - .4 — 2.3 μ SEC
β2 - 2.4 — 4.3 μ SEC
β3 - 4.4 - 6.3 μ SEC
β4 - 6.4 - 8.4 μ SEC
S = SCALER
BLOCK DIAGRAM – ELECTRONICS
MU 1864

Fig. 5

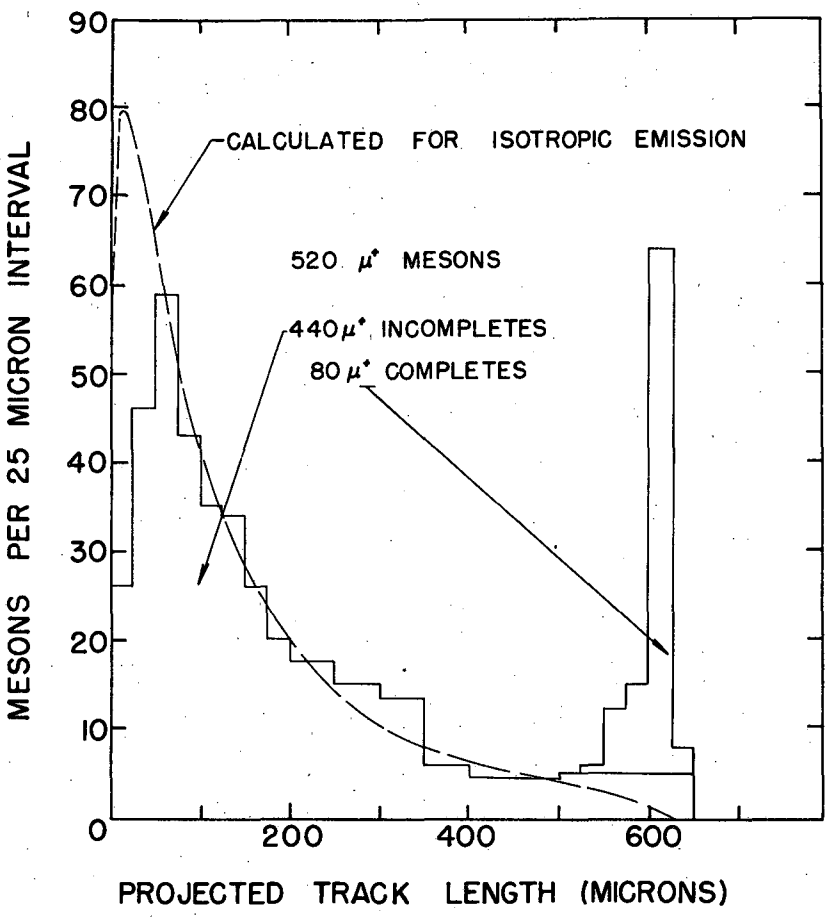
90
80
70
60
50
40
30
20
10
0
200
400
600
MESONS PER 25 MICRON INTERVAL
PROJECTED TRACK LENGTH (MICRONS)
CALCULATED FOR ISOTROPIC EMISSION
520 μ* MESONS
440μ* INCOMPLETES
80 μ* COMPLETES
MU3356

Fig. 6

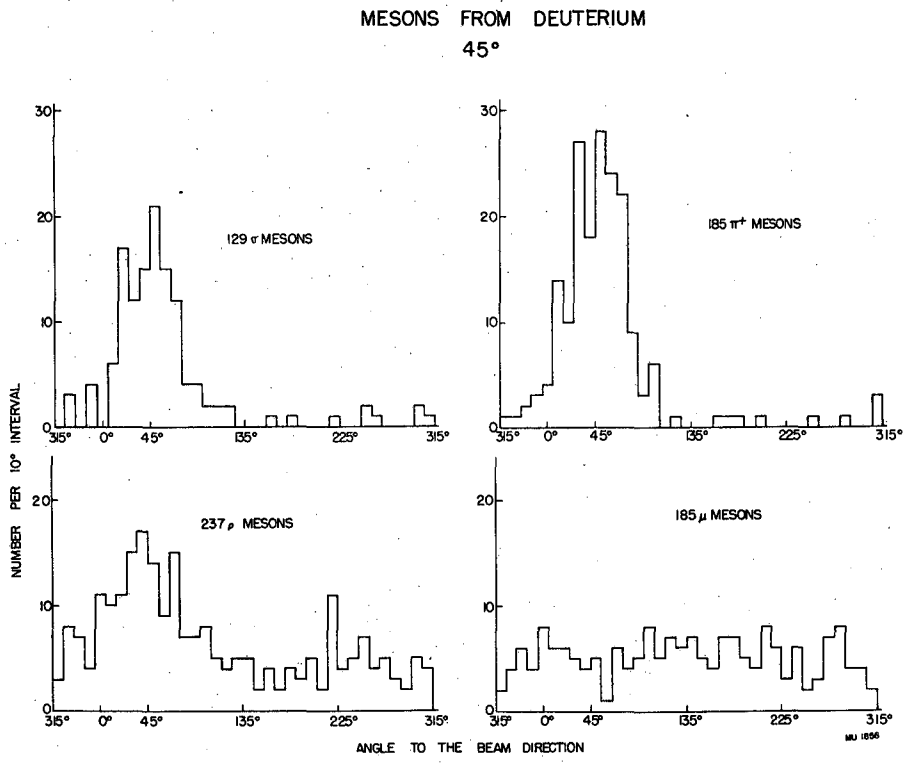
MESONS FROM DEUTERIUM
45°
129 σ MESONS
185 π+ MESONS
237 ρ MESONS
185 μ MESONS
NUMBER PER 10° INTERVAL
ANGLE TO THE BEAM DIRECTION
315° 0° 45° 135° 225° 315°
0 10 20 30

Fig. 7

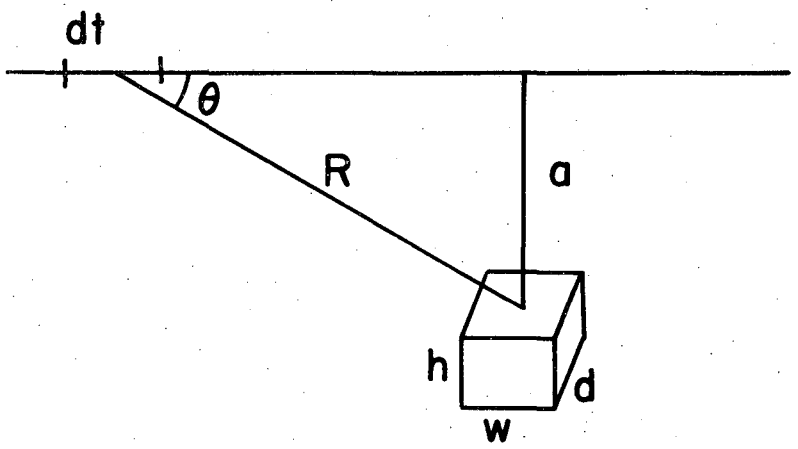

MU 33 55

Fig. 3

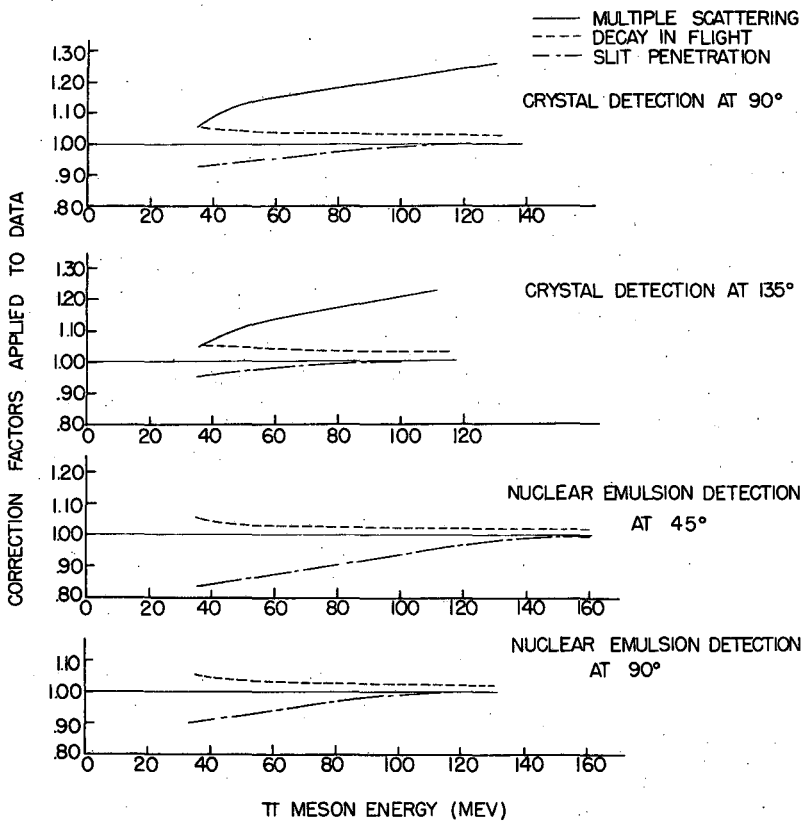
MULTIPLE SCATTERING
DECAY IN FLIGHT
SLIT PENETRATION
CRYSTAL DETECTION AT 90°
CRYSTAL DETECTION AT 135°
NUCLEAR EMULSION DETECTION AT 45°
NUCLEAR EMULSION DETECTION AT 90°
CORRECTION FACTORS APPLIED TO DATA
TT MESON ENERGY (MEV)
MU 1852

Fig. 9

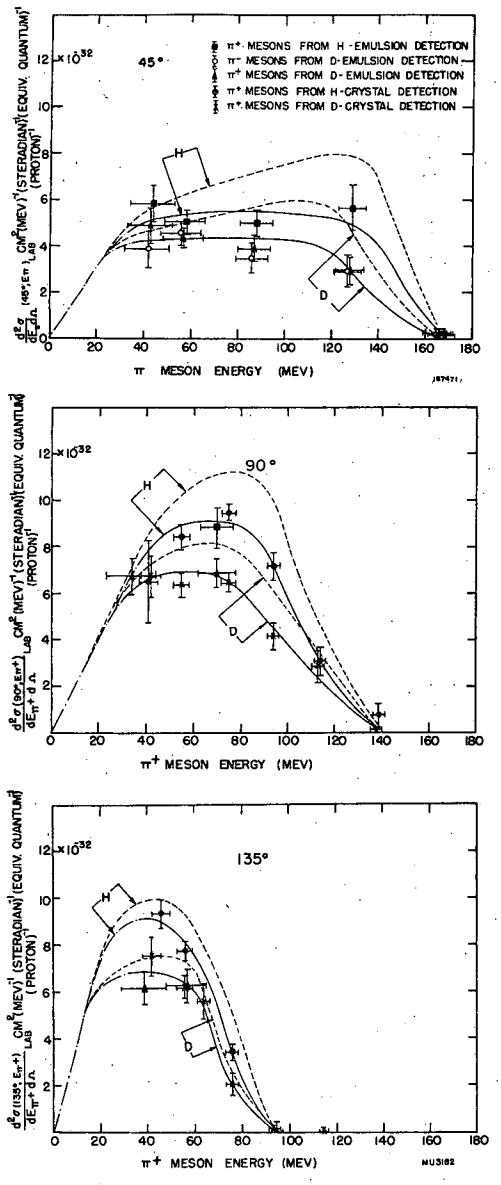
π+ MESONS FROM H - EMULSION DETECTION
π- MESONS FROM D-EMULSION DETECTION
π+ MESONS FROM D - EMULSION DETECTION
π+ MESONS FROM H-CRYSTAL DETECTION
π+ MESONS FROM D-CRYSTAL DETECTION
45°
90°
135°
H
D
π MESON ENERGY (MEV)
π+ MESON ENERGY (MEV)
(EQUIV. QUANTUM)
(STERADIAN)
(PROTON)
MU3162

Fig. 10

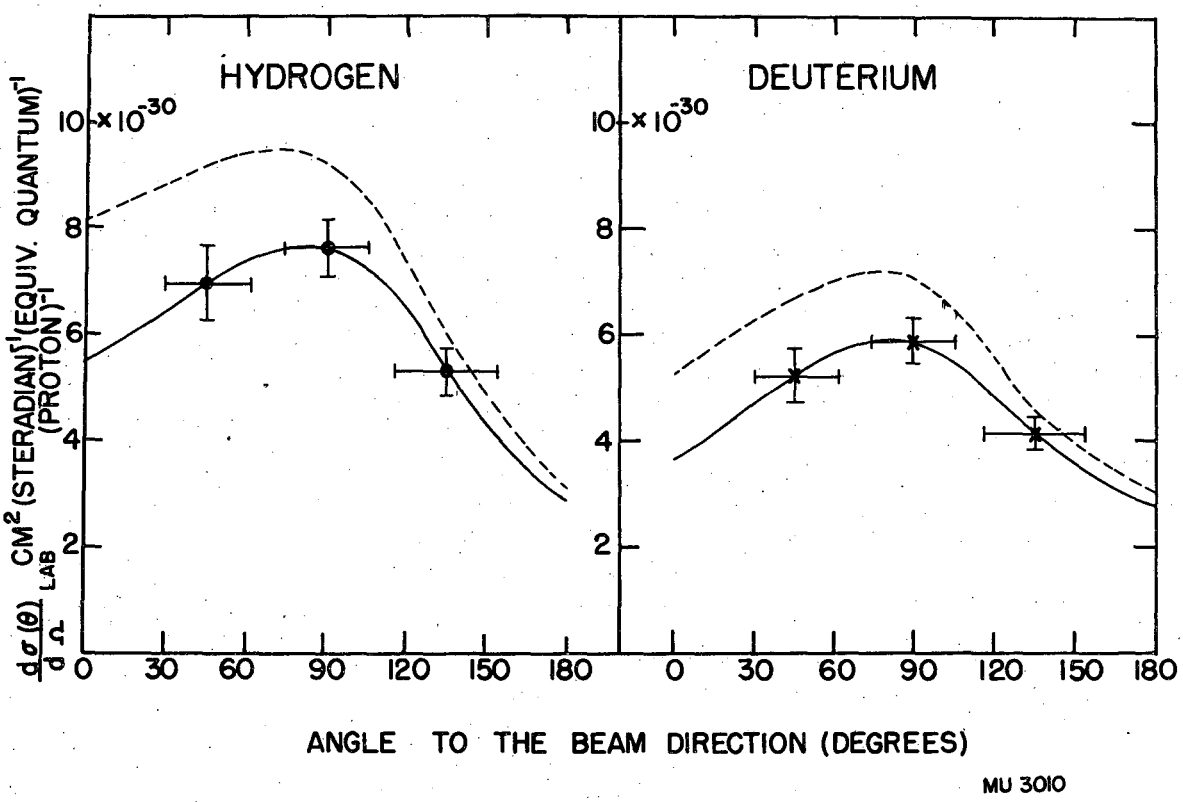
HYDROGEN
DEUTERIUM
10 x 10⁻³⁰
8
6
4
2
0
30
60
90
120
150
180
dσ(θ)/dΩ LAB CM² (STERADIAN)⁻¹ (EQUIV. QUANTUM)⁻¹ (PROTON)⁻¹
ANGLE TO THE BEAM DIRECTION (DEGREES)
MU 3010

Fig. 11

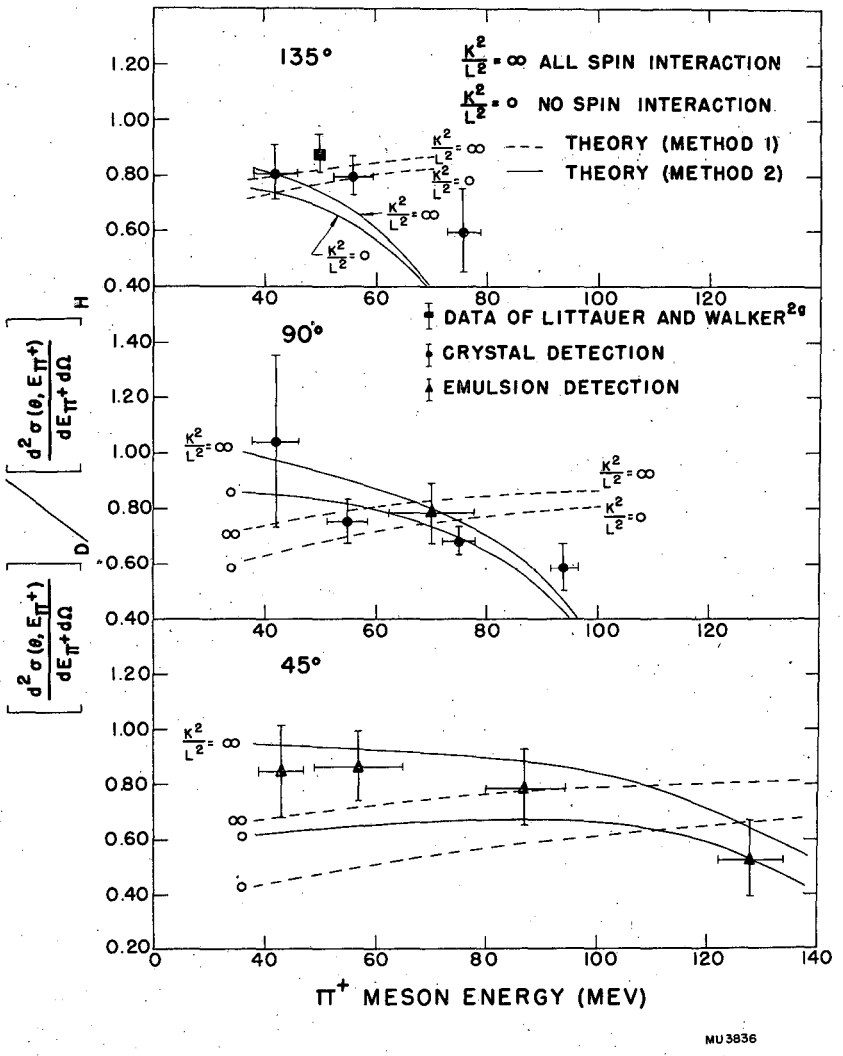
135°
90°
45°
$\frac{K^2}{L^2}=\infty$ ALL SPIN INTERACTION
$\frac{K^2}{L^2}=0$ NO SPIN INTERACTION
THEORY (METHOD 1)
THEORY (METHOD 2)
DATA OF LITTAUER AND WALKER[29]
CRYSTAL DETECTION
EMULSION DETECTION
$\left[\frac{d^2\sigma(\theta,E_{\pi^+})}{dE_{\pi^+}d\Omega}\right]_H \Big/ \left[\frac{d^2\sigma(\theta,E_{\pi^+})}{dE_{\pi^+}d\Omega}\right]_D$
π^+ MESON ENERGY (MEV)
MU3836

Fig. 12

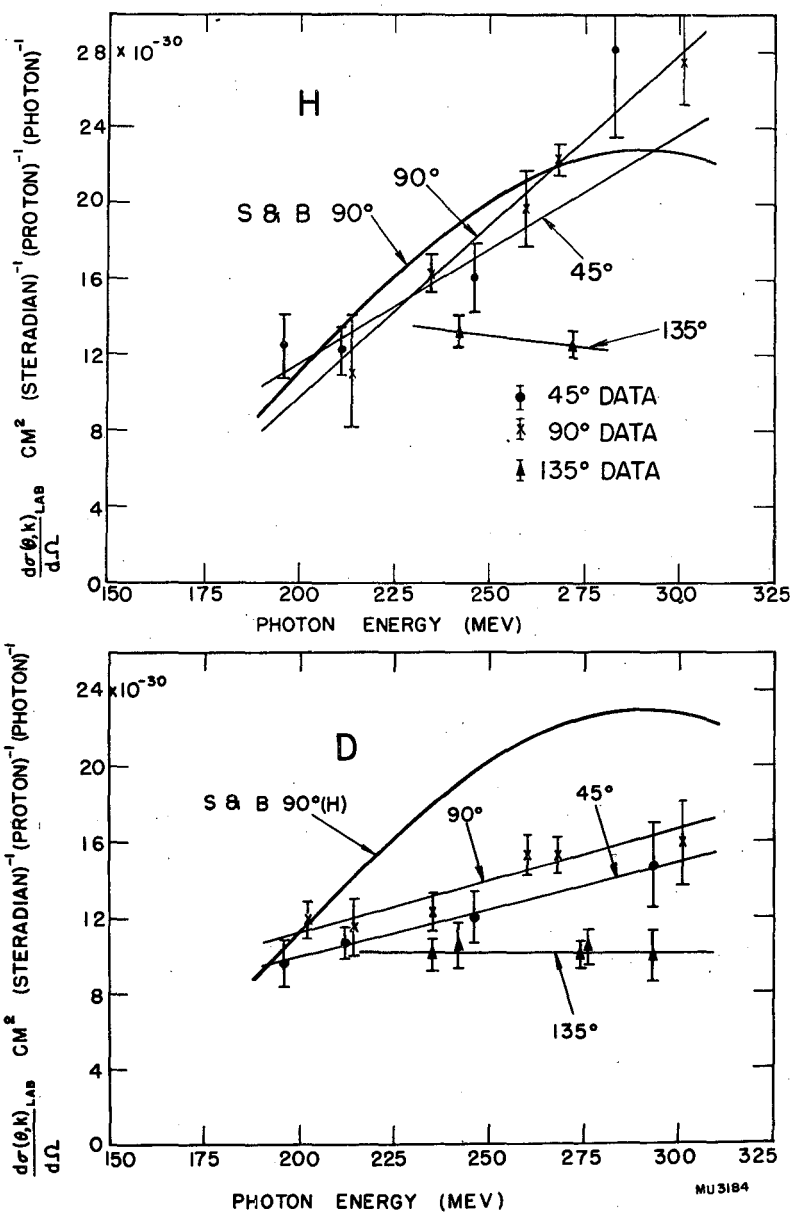
H
28 x 10^-30
24
20
16
12
8
4
0
S & B 90°
90°
45°
135°
45° DATA
90° DATA
135° DATA
dσ(θ,k)/dΩ LAB CM² (STERADIAN)⁻¹ (PROTON)⁻¹ (PHOTON)⁻¹
150
175
200
225
250
275
300
325
PHOTON ENERGY (MEV)
D
24 x 10^-30
20
16
12
8
4
0
S & B 90°(H)
90°
45°
135°
dσ(θ,k)/dΩ LAB CM² (STERADIAN)⁻¹ (PROTON)⁻¹ (PHOTON)⁻¹
150
175
200
225
250
275
300
325
PHOTON ENERGY (MEV)
MU3184

Fig. 13

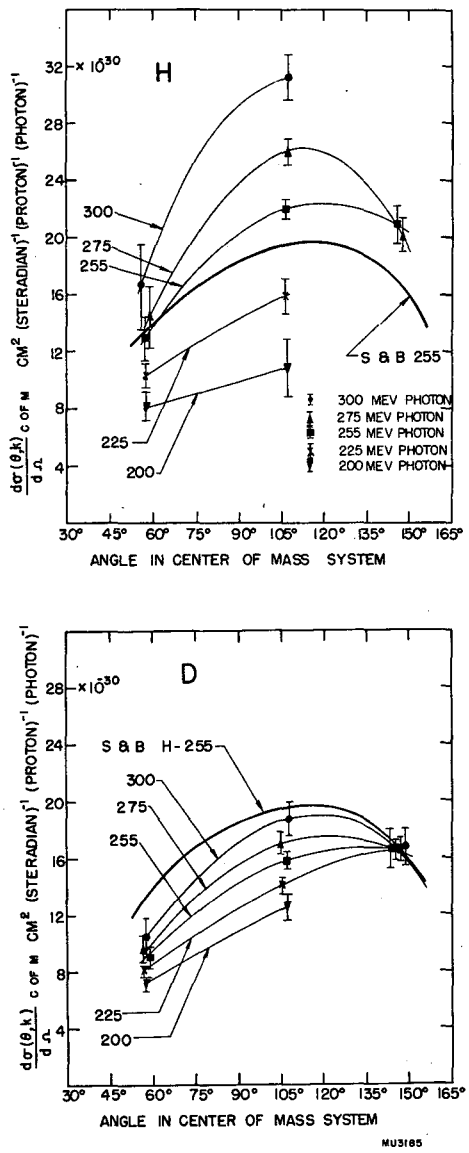
H
× 10⁻³⁰
300
275
255
225
200
S & B 255
300 MEV PHOTON
275 MEV PHOTON
255 MEV PHOTON
225 MEV PHOTON
200 MEV PHOTON
ANGLE IN CENTER OF MASS SYSTEM
D
S & B H-255
MU3185

Fig. 14